Optimal Electric Bus Charging Scheduling for Local Balancing of Fluctuations in PV Generation

Jakub Szcześniak, Tobias Massier, Marc Gallet
Electrification Suite and Test Lab,
TUMCREATE Ltd.,
Singapore

Anurag Sharma
Dept. of Electrical and Power Engineering,
Newcastle University International,
Singapore

***Abstract*—Photovoltaic power generation and charging of electric vehicles each pose a burden to distribution grids. Controlled charging of electric vehicles can mitigate the fluctuations of photovoltaics and ensure smoother grid operation. This paper presents an optimisation method to adjust the charging power of electric buses to respond to fluctuations from photovoltaic generation. In a case study, the method is applied to electric buses in Singapore using solar irradiance data and operation data of the whole public bus fleet, both in high resolution. Results show that optimal charging of electric public buses considerably smooths the grid load, while leading only to a minor cost increase.**

***Index Terms*—electric vehicles, photovoltaics, electric buses, optimisation**

NOMENCLATURE

n	Charger ID
b	Bus ID unique to each bus journey
t	Time of day (min)
p	Current time block
$\mathcal{N}$	Set of all chargers n
$\mathcal{B}$	Set of all bus journeys b
$\mathcal{T}$	Set of all time steps t
$\mathcal{P}$	Set of all time blocks p
$\mathcal{B}(p)$	Set of all bus journeys b in block p
$\mathcal{T}(p)$	Set of all time steps t in block p
Δt	Duration of one time step (min)
$t_{start}(p)$	Time of day when block p starts (min)
$t_{end}(p)$	Time of day when block p ends (min)
$t_{idle,start}(b)$	Time of day when bus b starts idling (min)
$t_{idle,end}(b)$	Time of day when bus b stops idling (min)
$t_{req}(b)$	Minimum required charging time of bus b
$c(n,b,t)$	Binary variable indicating whether charger n is occupied by bus b at time t
$Q(n,b)$	Binary variable indicating whether bus b is assigned to charger n
$z(b,t)$	Binary variable introduced to ensure that each bus b is connected continuously to a charger within each time block p
$y(b,t)$	Binary variable indicating whether bus b occupies a charger at time t
$X(b,t)$	Binary variable indicating whether bus b is charged with 150 kW at time t
$Y(b,t)$	Binary variable indicating whether bus b is charged with 300 kW at time t
$Z(b,t)$	Binary variable indicating whether bus b is charged with 450 kW at time t
$P_{ch}(b,t)$	Charging power of bus b at time t (W)
$P_{grid}(b,t)$	Fraction of $P_{ch}(b,t)$ supplied by the grid (W)
$P_{PV}(b,t)$	Fraction of $P_{ch}(b,t)$ supplied by PV (W)
$E_{init}(b)$	Initial energy capacity of the battery of bus b at its beginning of life (Wh)
$E_{EoL}(b)$	Energy capacity of the battery of bus b at its end of life (Wh)
$E_{req}(b)$	Energy that needs to be delivered to the battery of bus b to reach 90 % state of charge (Wh)
$SOC_{max}(b)$	Maximum battery state of charge of bus b
$SOC_{arr}(b)$	State of charge of the battery of bus b when it arrives at the terminus
η_{ch}	Efficiency of the charging process
$P_{ch,tot}(t)$	Total charging power at time t (W)
$P_{grid,tot}(t)$	Total power withdrawn from grid at time t (W)
$P_{PV,tot}(t)$	Total power generated by PV at time t (W)
$c_{el}(t)$	Price of electricity at time t (SGD/Wh)
$c_{ageing}(b,t)$	Ageing cost of the battery of bus b at time t (SGD)
$f_{150/300/450}$	Energy fade of a battery depending on the charging power (Wh/cycle)
c_{batt}	Battery cost (SGD)
$r_{ch/dis}$	Share of the impact of charging half-cycle on battery ageing during charging-discharging cycle

I. INTRODUCTION

Unlike fossil fuel power plants, renewable power generation such as solar photovoltaics (PV) or wind power is subject to weather conditions. Resulting power intermittency affects grid operation and stability. With over 400 GW of installed solar PV capacity globally by the end of 2017 [1], the majority is installed on distribution grid level such that even smaller installations can significantly jeopardise local grid operation.

This work was financially supported by the Singapore National Research Foundation under its Campus for Research Excellence And Technological Enterprise (CREATE) programme. The authors express their gratitude to the Solar Energy Research Institute of Singapore for the provision of solar irradiance data for Singapore.

There are various solutions to smooth out the power fluctuations caused by the intermittency, including local demand side management, battery or flywheel storage systems. Many methods to use stationary storage can be found in the literature, often combined with forecasting techniques. In [2], storage is used to limit the ramp rate of PV generation. A control strategy for a system including PV, battery storage and a supercapacitor is presented in [3], whereas [4] presents a control strategy with PV and battery storage in a DC micro-grid. A framework comprising day-ahead scheduling of energy demand and PV supply and incentives is introduced in [5].

In densely developed areas, limited space and high prices of land call for alternative solutions. The growing number of electric vehicles (EVs) offers additional battery storage capacity, particularly in urban areas. Strategies that employ EVs are presented in [6] and [7] while plugin-hybrid EVs are used in [8] and [9]. However, the available storage capacity of EVs is subject to their mobility patterns. Consequently, existing literature on balancing of PV using EVs often includes stationary storage systems to support the EV batteries.

Using EVs for grid balancing poses additional challenges. Firstly, the owners of private EVs might be reluctant to offer their batteries for grid purposes due to range anxiety and battery degradation. Secondly, the low battery capacity of passenger cars requires a high number of owners of EVs to be involved in order to accumulate a high storage capacity. The solution proposed in this paper overcomes those issues by using public electric buses for smoothing out PV fluctuations.

There are multiple advantages of using batteries of electric buses rather than of private EVs. As batteries of buses are of large capacity, they offer more flexibility per vehicle. Public buses operate on fixed schedules making their availability for charging and the energy needs more predictable. With only two parties involved, bus operator and grid operator are more likely to find an agreement to share the additional costs caused by using the bus batteries. Additionally, the deployment of electric buses can happen much faster than that of private EVs since it depends mainly on bus operators or local governments. In Shenzhen, for example, the public bus fleet was fully electrified within five years, from 277 electric buses in 2012 to over 16,000 in 2017 [10]. Other cities are also increasingly turning to electrified public transport [11].

In this paper, we propose a method to adjust the charging power of electric buses at termini or in depots such that it locally smooths out the fluctuations of PV generation. This method minimises fluctuations in grid load without compromising the bus schedule. A cost analysis is performed to determine the additional cost for balancing PV fluctuations. The method is applied in a case study of Singapore, a city state in a tropical region with low spatial smoothing effects for PV generation. Cloud evolution and motion in the region often cause sudden fluctuations in irradiance or widespread irradiance loss in minutes. Due to the small size of the country and absence of wind, PV is the only viable source of renewable energies in Singapore. PV installations exist on rooftops and facades of buildings, and on floating islands. The installed capacity is to increase significantly in the coming years. Singapore is also planning to electrify its large public bus fleet of more than 5000 buses in the near future, which will offer a huge amount of storage capacity. The model description is presented in Section II. In Section III, the model is demonstrated in a case study of Singapore. Section IV concludes the paper.

II. Model description

In this section, a two-stage optimisation model for balancing fluctuations in PV power generation is described. In stage I, the assignment of chargers to buses is optimised throughout the day. In stage II, the PV power fluctuations are balanced by optimising the charging power of the buses. The model is formulated as a mixed-integer linear programming problem and solved using Gurobi. The length of the time steps is 1 min and the studied period is one day.

A. System model

Each bus terminus is modelled and analysed individually. The analysis is based on a reconstruction of all journeys of public buses including their arrival and departure times. In order to determine the energy requirements and charging demand, a longitudinal dynamics model for electric buses elaborated in [12] is used. The bus arrival and departure time at each bus stop and the bus route information are derived from a historical real-world data set of the bus transaction records of passengers' trip fares. Charging of the buses is assumed to be performed via a state-of-the-art roof-mounted conductive charging system which provides charging power in discrete levels of 150 kW, 300 kW and 450 kW. The potential PV generation is estimated for each terminus based on historical irradiance data. The area of solar panels is chosen equal to the area of the roof that could cover the terminus. The performance factor and efficiency are chosen as $g = 75\,\%$ and $\eta_{PV} = 18\,\%$, respectively. The PV generation profile at time t is determined according to Equation (1), where $P_{PV,tot}$ is the output power in W, ϕ the solar irradiance in $\mathrm{W/m^2}$, and A the area in $\mathrm{m^2}$.

$$P_{PV,tot}(t) = \phi(t) \cdot A \cdot g \cdot \eta_{PV} \tag{1}$$

B. Stage I – Assignment of chargers to buses

The aim of the optimisation performed in stage I is to assign chargers to buses throughout the day such that each bus is connected to a charger for at least the minimum time it requires for charging. Furthermore, in order to provide flexibility to the charging process, the time that each bus is connected to a charger needs to be maximised. Given a limited number of chargers at each terminus, stage I optimisation ensures that the chargers are fully utilised and that there is a bus connected to every charger at all possible times.

In order to make the occupancy scheduling optimisation problem less computationally expensive and ensure the possibility to easily accommodate for unexpected changes caused by traffic conditions, the scheduling is divided into blocks of 30 min. Each 30-minute block is optimised separately. The minimum required charging time assumes charging with the

highest possible power of 450 kW. For each bus charging event, the amount of energy that is required is defined with the assumption that each bus needs to be recharged to a state of charge (SOC) of 90 % before the next departure. The derivation is shown in Equation (2) with $t_{req}(b)$ being the minimum required time, $E_{req}(b)$ the required amount of energy by bus b and η_{ch} the efficiency of the charging process.

$$t_{req}(b) = \frac{E_{req}(b)}{450\ \text{kW} \cdot \eta_{ch}} \tag{2}$$

All the variables are defined separately for each bus terminus and per 30-minute block. For each bus journey b, the input data for the optimisation are $t_{idle,start}(b)$, $t_{idle,end}(b)$ and $t_{req}(b)$. The idling start time $t_{idle,start}(b)$ indicates the earliest time a bus can start charging and the idling end time $t_{idle,end}(b)$ indicates the latest time a bus must stop charging.

1) Objective function: The objective function $f_1(p)$ aims at maximising the cumulative occupancy of the chargers $y(b,t)$ during time block p to provide flexibility of the charging power and time for each bus. The objective function which is to be maximised is defined for all $p \in \mathcal{P}$, where $\mathcal{P}$ is the set of all 30-minute blocks, and given as follows:

$$f_1(p) = \sum_{b \in \mathcal{B}(p)} \sum_{t \in \mathcal{T}(p)} y(b,t), \tag{3}$$

with $\mathcal{B}(p)$ being the set of all bus journeys b in block p and $\mathcal{T}(p)$ the set of all time steps t in block p.

2) Variables and constraints: The constraints applied to this problem ensure that the assignment process is performed according to operational requirements. They are defined for all $p \in \mathcal{P}$.

$$\forall n \in \mathcal{N}, \forall t \in \mathcal{T}(p): \quad \sum_{b \in \mathcal{B}(p)} c(n,b,t) \leq 1 \tag{4}$$

$$\forall b \in \mathcal{B}(p): \quad \sum_{n \in \mathcal{N}} \sum_{t=t_{idle,start}(b)}^{t_{idle,end}(b)} c(n,b,t) \geq t_{req}(b) \tag{5}$$

$$\forall b \in \mathcal{B}(p): \quad \sum_{n \in \mathcal{N}} \sum_{t=t_{start}(p)}^{t_{idle,start}(b)} c(n,b,t) = 0 \tag{6}$$

$$\forall b \in \mathcal{B}(p): \quad \sum_{n \in \mathcal{N}} \sum_{t=t_{idle,end}(b)}^{t_{end}(p)} c(n,b,t) = 0 \tag{7}$$

$$\forall n \in \mathcal{N}, \forall b \in \mathcal{B}(p): \quad \sum_{t \in \mathcal{T}(p)} c(n,b,t) \geq Q(n,b) \tag{8}$$

$$\forall n \in \mathcal{N}, \forall b \in \mathcal{B}(p): \quad \sum_{t \in \mathcal{T}(p)} c(n,b,t) \leq Q(n,b) \cdot M \tag{9}$$

$$\forall b \in \mathcal{B}(p): \quad \sum_{n \in \mathcal{N}} Q(n,b) \leq 1 \tag{10}$$

$$\forall b \in \mathcal{B}(p), \forall t \in \mathcal{T}(p): \quad \sum_{n \in \mathcal{N}} c(n,b,t) = y(b,t) \tag{11}$$

$$\forall b \in \mathcal{B}(p), \forall t \in \mathcal{T}(p): \quad y(b,t) + y(b,t-1) \geq z(b,t) \tag{12}$$

$$\forall b \in \mathcal{B}(p), \forall t \in \mathcal{T}(p): \quad y(b,t-1) - y(b,t) \leq z(b,t) \tag{13}$$

$$\forall b \in \mathcal{B}(p), \forall t \in \mathcal{T}(p): \quad y(b,t) - y(b,t-1) \leq z(b,t) \tag{14}$$

$$\forall b \in \mathcal{B}(p), \forall t \in \mathcal{T}(p): \quad 2 - y(b,t-1) - y(b,t) \geq z(b,t) \tag{15}$$

$$\forall b \in \mathcal{B}(p): \quad \sum_{t \in \mathcal{T}(p)} z(b,t) \leq 2 \tag{16}$$

Constraint (4) ensures that each charger n can be assigned to only one bus b at time t. Constraint (5) states that a bus b must occupy the charger for at least the minimum time $t_{req}(b)$. Constraints (6) and (7) state that a bus can only occupy a charger when it is idling at the terminus and therefore is not assigned to any charger before it comes to the terminus and after it leaves. Constraints (8) to (10) ensure that each bus is assigned to only one charger during each time block p. Constraints (8) and (9) indicate whether bus b is assigned to charger n ($Q(n,b) = 1$) or not ($Q(n,b) = 0$). A number $M = 1440$ equal to the number of time steps (minutes) during the day is used in Equation (9) to ensure a feasible solution. Constraint (10) ensures that for a given bus no more than one charger is assigned during each time block p. The remaining constraints (11) to (16) assure that each vehicle occupies a charger continuously within each time block p. They define that there are maximum two changes in the occupancy profile of the charger n by bus b, from not occupying to occupying (0 to 1) and from occupying to not occupying (1 to 0). Constraint (11) specifies the occupancy profile of each bus b over time. Constraints (12) to (15) are used to perform a bit-wise XOR operation on the occupancy profile and its shifted copy. Constraint (16) ensures that the sum of the bits in the result of the bit-wise operation over all time steps t for each bus b is less or equal to two.

C. Stage II – PV balancing

From stage I, we obtain the occupancy schedule indicated by variable $y(b,t)$. This is used in stage II to determine the time frame when each bus is connected to a charger and delimits the duration when the charging process can take place. In this stage, the charging strategy for a bus terminus with locally installed PV generation is optimised. It aims at using all of the generated PV power to charge buses while balancing fluctuations locally in order to reduce the negative impact on the grid. Grid power fluctuations are defined through the changes in the absolute value of the power withdrawn from the grid between two consecutive time steps. They are modelled using the balancing term $bal(t)$ defined in Equation (17).

$$\forall t \in \mathcal{T}: \quad bal(t) = \left| P_{grid,tot}(t) - P_{grid,tot}(t-1) \right| \tag{17}$$

1) Objective function: The objective function f_2 that has to be minimised is given as follows:

$$f_2 = \sum_{t \in \mathcal{T}} bal(t) \tag{18}$$

The objective function ensures not only balancing of PV generation but also a lower number of changes in the grid load when PV generation is zero. Hence, it ensures smoothing of the charging profile of electric buses at a terminus as well.

2) Variables and constraints: The constraints related to the physical energy and charging requirements of the buses, subject to the available charging power levels and state of the batteries, are defined as follows:

$$\begin{aligned}\forall b \in \mathcal{B}, \forall t \in \mathcal{T}: \\ P_{ch}(b,t) = \big[X(b,t)\cdot 150 \; + \; Y(b,t)\cdot 300 \\ + \; Z(b,t)\cdot 450\big]\cdot 10^3 \cdot y(b,t)\end{aligned} \tag{19}$$

$$\forall b \in \mathcal{B}, \forall t \in \mathcal{T}: \quad X(b,t) + Y(b,t) + Z(b,t) \leq 1 \tag{20}$$

$$\forall b \in \mathcal{B}, \forall t \in \mathcal{T}: \; P_{ch}(b,t) = P_{grid}(b,t) + P_{PV}(b,t) \tag{21}$$

$$\forall b \in \mathcal{B}: \; E_{req}(b) = \big(SOC_{max}(b) - SOC_{arr}(b)\big)\cdot E_{init}(b) \tag{22}$$

$$\forall b \in \mathcal{B}: \; \sum_{t\in\mathcal{T}} P_{ch}(b,t)\cdot \Delta t \cdot \eta_{ch} \geq E_{req}(b) \tag{23}$$

$$\forall b \in \mathcal{B}: \sum_{t\in\mathcal{T}} P_{ch}(b,t)\cdot \Delta t \cdot \eta_{ch} \leq E_{req}(b) + P_{min}\cdot \Delta t \cdot \eta_{ch} \tag{24}$$

$$\forall t \in \mathcal{T}: \quad P_{ch,tot}(t) = \sum_{b\in\mathcal{B}} P_{ch}(b,t) \tag{25}$$

$$\forall t \in \mathcal{T}: \quad P_{grid,tot}(t) = \sum_{b\in\mathcal{B}} P_{grid}(b,t) \tag{26}$$

$$\forall t \in \mathcal{T}: \quad P_{PV,tot}(t) = \sum_{b\in\mathcal{B}} P_{PV}(b,t) \tag{27}$$

$$\forall b \in \mathcal{B}, \forall t \in \mathcal{T}: \quad P_{grid}(b,t) \geq 0 \tag{28}$$

$$\forall b \in \mathcal{B}, \forall t \in \mathcal{T}: \quad P_{PV}(b,t) \geq 0 \tag{29}$$

Constraints (19) and (20) provide a choice of charging power between 150 kW, 300 kW and 450 kW and ensure that charging only occurs when a bus occupies a charger. This is enforced by multiplying the power with variable $y(b,t)$, which results from stage I of the optimisation. Constraint (21) defines the power balance: the power supplied to a bus consists of power withdrawn from the grid and power generated by PV. In Constraint (22), the energy required by the battery of each bus b is defined. The value of SOC_{max} is set to 90 % in this study. Constraints (23) and (24) specify the minimum and maximum energy which should be delivered to the battery of each bus b in Wh. They effectively assure that the state of charge after charging is equal to at least 90 % of the battery capacity but not greater than 90 % plus the energy that can be supplied by the minimum possible power of P_{min} = 150 kW within one time step Δt. The efficiency η_{ch} of the charging process is assumed to be 93 %. Equations (25) and (26) describe the total charging power and grid power in each time step respectively and Equation (27) ensures that the PV power is fully utilised on-site. Constraints (28) and (29) specify that grid power and PV power are always positive, which means that no power flow from the buses to the grid is allowed.

D. Operating cost optimisation

Another optimisation objective studied in this work aims at minimising the overall operating cost. To that end, the previous objective function for stage II (f_2, Equation (18)) is replaced by f_3 defined in Equation (30). The total operating cost is expressed as the sum of electricity cost and battery ageing cost.

$$f_3 = \sum_{t\in\mathcal{T}} \left(P_{ch,tot}(t)\cdot \Delta t \cdot c_{el}(t) + \sum_{b\in\mathcal{B}} c_{ageing}(b,t) \right) \tag{30}$$

The battery ageing cost $c_{ageing}(b,t)$ is defined in Equation (31), based on the principles described in [13].

$$\begin{aligned}c_{ageing}(b,t) = \Bigg(\frac{X(b,t)\cdot f_{150} + Y(b,t)\cdot f_{300} + Z(b,t)\cdot f_{450}}{E_{init}(b) - E_{EoL}(b)} \\ \cdot c_{batt}\cdot r_{ch/dis}\cdot \frac{P_{ch}(b,t)\cdot \Delta t}{E_{init}(b)} \Bigg), \forall b \in \mathcal{B}, \forall t \in \mathcal{T}\end{aligned} \tag{31}$$

In Equation (31), f_{150}, f_{300} and f_{450} represent the energy fade per cycle expressed in Wh/cycle for charging powers of 150 kW, 300 kW and 450 kW respectively. It is pro-rated over the total life cycle energy fade. The latter is defined as the difference between the initial beginning-of-life energy content of the battery, $E_{init}(b)$, and the end-of-life energy content, $E_{EoL}(b)$, defined as 80 % of $E_{init}(b)$ [14]. This share of the energy content fade of one full cycle is multiplied by the battery cost c_{batt}. Since the energy fade f is defined for one full cycle which includes charging and discharging and we only model the ageing caused by the charging process, a factor $r_{ch/dis}$ needs to be included. It represents the share of ageing of the battery which happens only during charging as opposed to a full charging and discharging cycle. Furthermore, since the charging power can be modified during charging, the share of each time step in the ageing cost of full charging process needs to be accounted for. It is done by multiplying the ageing cost during full charging process by the energy share delivered during each time step.

In the optimisation, the battery size is assumed to be 150 kWh and the energy fading of the batteries is approximated based on [13] and [15] to f_{150} = 6.25 Wh/cycle, f_{300} = 6.70 Wh/cycle and f_{450} = 7.23 Wh/cycle for the chosen battery. The specific battery price is set to SGD 250/kWh [16] and the resale value of the depleted battery for second life applications is set to 20 % of its initial value [17]. Therefore, c_{batt} is calculated by subtracting the resale value from the price of a new battery. The charging process is assumed to contribute 50 % to the ageing during the whole charge-discharge cycle. Hence, the factor $r_{ch/dis}$ is assumed to be 0.5. For the following case study, the half-hourly price of electricity is taken from the website of the Energy Market Company in Singapore [18].

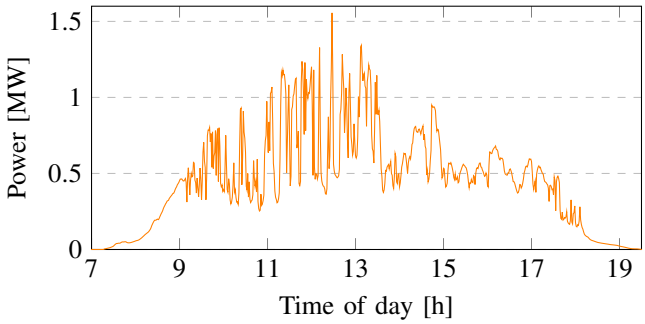

Fig. 1. PV power generation profile at Hougang bus interchange on a sunny day with high fluctuations in solar irradiance.

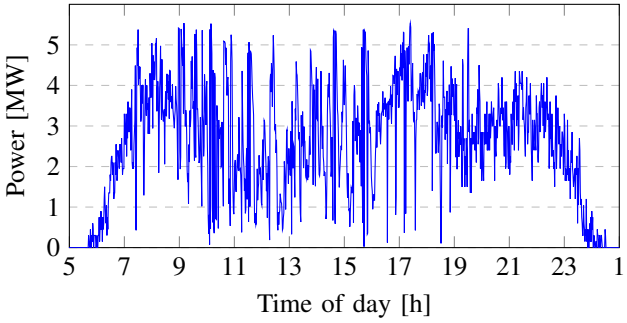

Fig. 2. Grid load at Hougang bus interchange resulting from uncontrolled charging.

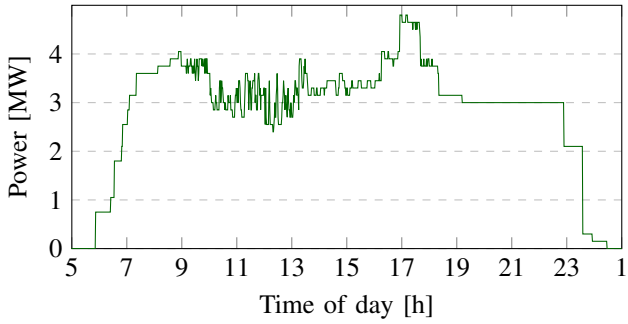

Fig. 3. Optimal charging profile at Hougang bus interchange in the presence of PV generation.

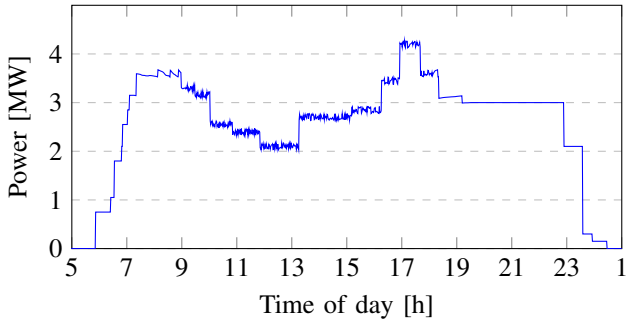

Fig. 4. Grid load at Hougang bus interchange resulting from the optimal charging profile shown in Fig. 3.

III. Case Study

Using the results presented in [12], the bus arrival and departure data for a major bus terminus in Singapore – Hougang bus interchange – comprising 1217 bus journeys have been extracted for a selected weekday. Charging happens over a period ranging from 5:35 a.m., when the first bus arrives at the terminus, until 12:32 a.m. of the next day, when the last bus leaves the terminus. The cumulative energy required for all buses in this data set is 55.4 MWh (sum of all $E_{req}(b)$, calculated with (22) using $SOC_{arr}(b)$ from the data set).

We choose historical irradiance data from a measurement station near the bus interchange for a sunny day with high fluctuations (Fig. 1). Three different charging scenarios are analysed and compared. In Scenario 1, the constraints of both stages of the model are fulfilled but no optimisation according to (18) or (30) is performed. In Scenario 2, grid balancing optimisation by minimising (18) is carried out. In Scenario 3, total operating cost is minimised according to (30).

As neither grid nor operating cost are considered in Scenario 1, the grid load is highly fluctuating due to charging of buses, as displayed in Fig. 2. In total, 56.7 MWh of energy are used for charging in this case. The total cost is SGD 7406 with electricity cost of SGD 5970 and ageing cost of SGD 1436.

Fig. 3 presents the optimised charging profile obtained in Scenario 2. The profile exhibits significant fluctuations – especially around noon – in order to counteract the fluctuations of the PV generation. In Fig. 4, the grid load which results from subtracting PV power from the charging profile is shown. Consequently, the curve is much smoother than in Fig. 2. The total operating cost for PV balancing is SGD 7368 with electricity cost of SGD 5936 and battery ageing cost of SGD 1432. The energy demand for charging amounts to 56.4 MWh.

The resulting grid load in Scenario 3 is displayed in Fig. 5. In this scenario, charging of the buses is preferred when the electricity price is low while also considering battery ageing. This can be observed in the morning and afternoon hours when the charging power alters due to significant changes in electricity price. For example, at 10 a.m., the electricity price increases and consequently, the charging power decreases. In this scenario, the total energy demand for charging is 55.4 MWh. The total cost amounts to SGD 7148 with electricity cost of SGD 5806 and battery ageing cost of SGD 1342. Battery ageing cost accounts for around 19 % of the operating cost. Compared to the findings presented in [13], this ageing cost factor has significantly decreased over the past years and can be attributed to lower price and extended life of batteries.

In the following paragraph, the specific costs c_s of charging and battery ageing per MWh for the three presented scenarios are compared. In Scenario 1, c_s = SGD 130.64/MWh. PV balancing (Scenario 2) yields a slightly lower value of SGD 130.55/MWh. Cost optimisation in Scenario 3 yields the lowest value of c_s = SGD 128.99/MWh. Compared to Scenario 3, c_s increases by approximately 1.3 % in Scenario 1 and 1.2 % in Scenario 2. This comparison does not include installation and operating cost of a PV balancing system.

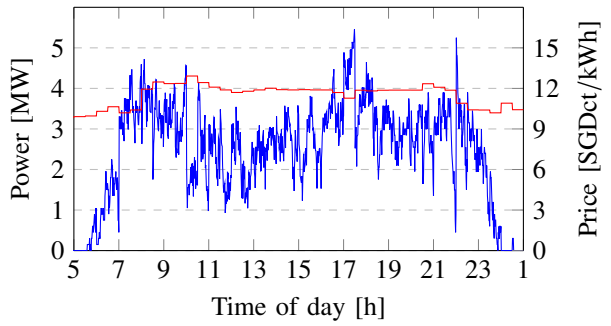

Fig. 5. Electricity price in SGDct (red) and grid load (blue) at Hougang bus interchange optimised to minimise total operating cost.

TABLE I
RESULTS OF CHARGING OPTIMISATION FOR DIFFERENT SCENARIOS.

Result	Scenario 1	Scenario 2	Scenario 3
C_{tot} (SGD)	7405.80	7368.10	7148.40
C_{el} (SGD)	5969.90	5936.10	5806.30
C_{ag} (SGD)	1435.90	1432.00	1342.10
E_{tot} (MWh)	56.69	56.44	55.42
E_{pv} (MWh)	5.73	5.73	5.73
E_{grid} (MWh)	50.96	50.71	49.69
c_s (SGD/MWh)	130.64	130.55	128.99
Δc (%)	1.28	1.21	0

However, the cost of high variations in grid load of up to more than 4 MW/min caused by charging that could jeopardise grid stability is not included in the price in this study either.

Cost and energy demand of all three scenarios are summarised in Table I. The total cost C_{tot} is the sum of electricity cost C_{el} and ageing cost C_{ag}, the energy demand E_{tot} is the sum of energy E_{pv} and E_{grid} provided by PV and the grid, c_s is the specific cost per MWh, and Δc is the relative cost difference in comparison to Scenario 3.

We repeated the study with different representative PV profiles and obtained similar results. The specific costs c_s were 1.2 % to 1.4 % higher in Scenarios 1 and 2 as compared to Scenario 3. When not enough buses were available to utilise available PV, our method could still reduce the fluctuations, leaving a smoother PV profile to be fed into the grid.

IV. CONCLUSION

In this paper, we presented a method for balancing fluctuations in solar PV using electric buses. This method is implemented by adjusting the charging power of the buses to even out the fluctuations and generate a smooth load profile. Compared to uncontrolled charging or the cost minimisation strategy, our solution considerably improves the stability of the local power grid. Operating costs increase only marginally when our method for balancing of PV fluctuations is applied. Furthermore, the cost of integrating highly fluctuating load profiles with ramps of up to 4 MW/min at a single interchange would lead to an increase of specific cost in Scenarios 1 and 3. However, the cost comparison would then also have to include installation and operating costs of a PV balancing system.

REFERENCES

[1] International Energy Agency, "Snapshot of global photovoltaic markets," 2018, accessed: 2019-02-27. [Online]. Available: http://www.iea-pvps.org/fileadmin/dam/public/report/statistics/IEA-PVPS%5f-%5fA%5fSnapshot%5fof%5fGlobal%5fPV%5f-%5f1992-2017.pdf

[2] R. van Haaren, M. Morjaria, and V. Fthenakis, "Utility scale PV plant variability and energy storage for ramp rate control," in *Proceedings of the 2013 IEEE 39th Photovoltaic Specialists Conference (PVSC)*. IEEE, Jun. 2013, pp. 973–979.

[3] S. Kumar Kollimalla, M. Mishra, and L. Narasamma N, "A new control strategy for interfacing battery supercapacitor storage systems for PV system," in *Proceedings of the 2014 IEEE Students' Conference on Electrical, Electronics and Computer Science, SCEECS 2014*, Mar. 2014, pp. 1–6.

[4] J. Umuhoza, Y. Zhang, S. Zhao, and H. A. Mantooth, "An adaptive control strategy for power balance and the intermittency mitigation in battery-PV energy system at residential DC microgrid level," in *Proceedings of the 2017 IEEE Applied Power Electronics Conference and Exposition (APEC)*, Mar. 2017, pp. 1341–1345.

[5] T. Sadamoto, T. Ishizaki, M. Koike, Y. Ueda, and J.-I. Imura, "Spatiotemporally multiresolutional optimization toward supply-demand-storage balancing under PV prediction uncertainty," *IEEE Transactions on Smart Grid*, vol. 6, pp. 853–865, Mar. 2015.

[6] F. Marra, G. Y. Yang, Y. T. Fawzy, C. Træholt, E. Larsen, R. Garcia-Valle, and M. Møller Jensen, "Improvement of local voltage in feeders with photovoltaic using electric vehicles," *IEEE Transactions on Power Systems*, vol. 28, no. 3, pp. 3515–3516, Aug. 2013.

[7] N. Liu, Q. Chen, J. Liu, X. Lu, P. Li, J. Lei, and J. Zhang, "A heuristic operation strategy for commercial building microgrids containing EVs and PV system," *IEEE Transactions on Industrial Electronics*, vol. 62, no. 4, pp. 2560–2570, Apr. 2015.

[8] M. J. E. Alam, K. M. Muttaqi, and D. Sutanto, "Effective utilization of available PEV battery capacity for mitigation of solar PV impact and grid support with integrated V2G functionality," *IEEE Transactions on Smart Grid*, vol. 7, no. 3, pp. 1562–1571, May 2016.

[9] E. Akhavan-Rezai, M. F. Shaaban, E. F. El-Saadany, and F. Karray, "Managing demand for plug-in electric vehicles in unbalanced LV systems with photovoltaics," *IEEE Transactions on Industrial Informatics*, vol. 13, no. 3, pp. 1057–1067, Jun. 2017.

[10] L. Lu, L. Xue, and W. Zhou, "How did Shenzhen, China build world's largest electric bus fleet?" Apr. 2018, accessed: 2019-02-26. [Online]. Available: https://www.wri.org/blog/2018/04/how-did-shenzhen-china-build-world-s-largest-electric-bus-fleet

[11] Bloomberg New Energy Finance, "Electric buses in cities: Driving towards cleaner air and lower CO_2," Bloomberg, Tech. Rep., Mar. 2018. [Online]. Available: https://data.bloomberglp.com/professional/sites/24/2018/05/Electric-Buses-in-Cities-Report-BNEF-C40-Citi.pdf

[12] M. Gallet, T. Massier, and T. Hamacher, "Estimation of the energy demand of electric buses based on real-world data for large-scale public transport networks," *Applied Energy*, vol. 230, pp. 344–356, Nov. 2018.

[13] A. E. Trippe, T. Massier, and T. Hamacher, "Optimized charging of electric vehicles with regard to battery constraints – case study: Singaporean car park," in *Proceedings of the 2013 IEEE EnergyTech*. IEEE, May 2013, pp. 1–6.

[14] D. Strickland, L. Chittock, D. A. Stone, M. P. Foster, and B. Price, "Estimation of transportation battery second life for use in electricity grid systems," *IEEE Transactions on Sustainable Energy*, vol. 5, pp. 795–803, Mar. 2014.

[15] Y. Wu, P. Keil, S. F. Schuster, and A. Jossen, "Impact of temperature and discharge rate on the aging of a LiCoO2/LiNi0.8Co0.15Al0.05O2 lithium-ion pouch cell," *Journal of The Electrochemical Society*, vol. 164, pp. A1438–A1445, May 2017.

[16] S. M. Knupfer, R. Hensley, P. Hertzke, P. Schaufuss, N. Laverty, and N. Kramer, "Electrifying insights: How automakers can drive electrified vehicle sales and profitability," Jan. 2017, accessed: 2019-02-18. [Online]. Available: https://www.mckinsey.com/industries/automotive-and-assembly/our-insights/electrifying-insights-how-automakers-can-drive-electrified-vehicle-sales-and-profitability

[17] I. Hartwell and J. Marco, "Management of intellectual property uncertainty in a remanufacturing strategy for automotive energy storage systems," *Journal of Remanufacturing*, vol. 6:3, Dec. 2016.

[18] Energy Market Company, "Price information," 2018, accessed: 2019-01-29. [Online]. Available: https://www.emcsg.com/marketdata/priceinformation